
Effects of viscoelasticity and time-dependent plasticity on nanoindentation measurements of human cortical bone

Zaifeng Fan,^{1*} Jae-Young Rho^{1,2}

¹Department of Biomedical Engineering, ET330, University of Memphis, Memphis, Tennessee 38152

²Department of Orthopaedic Surgery, University of Tennessee–Campbell Clinic, Memphis, Tennessee

Received 15 May 2002; revised 29 October 2002; accepted 21 November 2002

Abstract: The viscoelastic and time-dependent plastic effects on the nanoindentation measurement of osteonal lamella in a human cortical bone were investigated. The elastic modulus of osteonal lamella obtained from the quasi-static technique was strongly affected by the indentation rate and time-dependent plasticity. The effects of time-dependent plasticity can be diminished by multiple loading–unloading cycles and a long holding period at maximal load. After minimizing the contribution of time-dependent plasticity to

unloading data, it was surprisingly found that the elastic modulus was proportional to indentation strain rate raised to the 0.06 power, which is similar to conventional test results. © 2003 Wiley Periodicals, Inc. *J Biomed Mater Res* 67A: 208–214, 2003

Key words: nanoindentation; strain rate; viscoelasticity; plasticity; osteonal lamella; microstructure

INTRODUCTION

As a biological material, human cortical bone exhibits a complex microstructure and microcomponents, which result in complicated mechanical properties.^{1,2} Viscoelasticity is one of these properties. The primary components of bone are stiff, hydroxyapatite-like mineral and collagen. Because of the viscoelastic nature of collagen fibers in the bone matrix, bone itself has remarkable viscoelasticity.³ In compression tests, McElhaney⁴ found bone to be stiffer and stronger at higher strain rates. Carter and Hayes^{5,6} found that both strength and elastic modulus were approximately proportional to strain rate raised to the 0.06 power. This relationship was suggested to be true for all bones in the skeleton. However, most previous investigations regarding viscoelasticity were conducted at the macrostructural level with conventional mechanical testing methods, such as tension and compression testing. Because of the limitations of sample preparation and the availability of appropriate testing

methods,⁷ investigations of viscoelasticity of bone at the microstructural level are rare.

Nanoindentation is widely used for investigating the mechanical properties of thin films, small volumes, and microstructural features and has been proven to be an effective method.⁸ Nanoindentation techniques also have been used to study viscoelastic and creep-plastic properties of many materials. Flores and Calleja⁹ investigated the viscoelastic-plastic properties of polyethylene terephthalate with nanoindentation testing and found that the holding time at maximal load could affect both the elastic modulus and hardness. Turnbull and White¹⁰ found that the time-dependent plastic effects contributing to the initial portion of the unloading curve could lead to an unsatisfactory analysis. Lucas and Oliver¹¹ also investigated the effects of varied indentation strain rates on hardness. Pollock et al.¹² suggested that the indentation strain rate should be related to the strain rate determined by conventional tests.

Recently, nanoindentation has been used to investigate mechanical properties of bone at the microstructural level^{7,13–18}; however, nanoindentation experiments were conducted with various load-time functions. Because of the nature of viscoelasticity and time-dependent plasticity of bone material,¹⁹ it is believed that the load-time sequence affects nanoindentation measurements, but most previous studies did not take into account viscoelasticity and time-dependent plasticity.

*Current address: Orthopaedic & Rehabilitation Engineering Center, Marquette University, Milwaukee, WI 55201

Correspondence to: Z. Fan; e-mail: Zaifeng.Fan@Marquette.edu

Contract grant sponsor: The University of Memphis Faculty Research Grant; contract grant numbers: NIH45297, NSF DMR-0076497

The present study explored how the elastic modulus measured by nanoindentation is affected when different experimental procedures are applied. The relationship between indentation strain rate and elastic modulus was investigated to determine the effects of time-dependent properties (viscoelasticity and time-dependent plasticity) during nanoindentation measurements of osteonal lamellae in human cortical bone. The following hypotheses were tested: 1. the indentation rate affects the elastic modulus measured by nanoindentation; and 2. multiple loading-unloading cycles and different holding times at maximal loading level also affect the elastic modulus measured by nanoindentation.

MATERIALS AND METHODS

A bone sample was obtained from the midshaft of one human tibia (52 years old) without bone disease. After being dehydrated in air, specimens were then embedded in epoxy resin without infiltration at room temperature. The epoxy resin was used to provide support during tests and has no effect on test results as long as no indents are made close to the bone-resin boundary. After using silicon carbide abrasive papers with progressively finer grit sizes (600, 800, and 1200 grit) to grind the surfaces of the specimens, they were polished on microcloths with a 0.05- μm aluminum suspension.

A Triboindenter (Hysitron, Inc., Minneapolis, MN) was used to conduct all indentation tests. The system has load and displacement resolutions of 1 nN and 0.02 nm. The Oliver-Pharr method⁸ for determining the elastic modulus has been well documented and is not discussed here at length. The quantities of concern include the contact area A_c and the contact stiffness S . A Berkovich indenter was used in all experiments. The indentation modulus typically provides values that are similar to Young's modulus for the specimen material. The indentation modulus is found using:

$$E_s = \frac{1 - \nu_s^2}{\frac{1}{E_r} - \frac{1 - \nu_i^2}{E_i}} \quad (1)$$

where the subscripts s and i refer to the sample and the indenter, respectively. The elastic properties of the diamond indenter were: $\nu_i = 0.07$ and $E_i = 1140$ GPa. In this study, the Poisson's ratio of cortical bone was 0.3. For the specimen, E_r is the reduced modulus, which is found from the indentation test data and is given by:

$$E_r = \frac{\sqrt{\pi}}{2} \frac{S}{\sqrt{A_c}} \quad (2)$$

Although the contact area for a perfect Berkovich geometry is given by $A_c = 24.5h_c^2$, where h_c is contact depth, there are deviations from the Berkovich geometry because of blunting at the tip. The contact area can be estimated directly from the indentation load-displacement data. The process requires a precise knowledge of the shape of the indenter determined

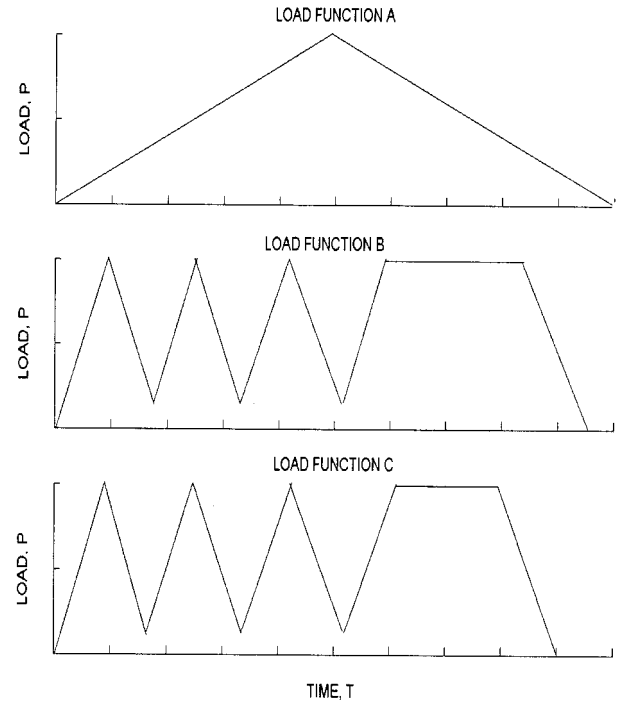


Figure 1. The load-time sequences; peak load = 6 mN for all functions. Indentation rate is varied for load functions A and B, whereas holding time is fixed (180 s) at load function B. Holding time is varied for function C, whereas indentation rate is fixed (300 $\mu\text{N/s}$).

in special calibration experiments and measurement of the plastic depth of the contact, referred to as the contact depth. The contact depth can be computed from the contact stiffness, the peak load, and the maximum depth of penetration, all of which are experimentally measurable from the load-displacement data. Thus, in the present study, the contact area calibrated by using the method described by Oliver and Pharr⁸ was used for all analyses.

Three load-time functions were used in the present study. The load-time sequences are shown in Figure 1.

- Simple loading-unloading with various indentation rates.
- Loading-unloading three times in succession followed by a final loading and then a fixed holding period of 180 s applied before final unloading with varied indentation rates.
- The same as function B, but with various holding periods with a fixed indentation rate of 300 $\mu\text{N/s}$.

The indentation rates used in function A and B were 10, 30, 50, 100, 300, 500, and 1000 $\mu\text{N/s}$. For function C, the different holding times at maximal loading were 10, 30, 100, 180, 300, 500, and 1000 s, and the indentation rate was kept at 300 $\mu\text{N/s}$. The 180-s holding period used in function B and the indentation rate of 300 $\mu\text{N/s}$ used in function C were chosen based on the middle range of the varied holding times and indentation rates. The peak load used in this study was kept constant at 6000 μN for all indents. Load function A provided information about the effect of indentation rate on the elastic modulus measurement. Multiple loading-unloadings were done in load functions B and C to

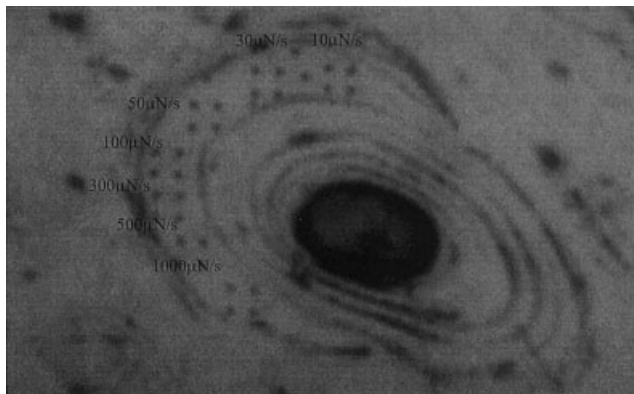


Figure 2. The optical micrograph of the indents produced from load function A.

determine whether deformation is reversible and whether the unloading data used for analysis purposes were mostly elastic.⁸ The holding period used in load functions B and C allowed any final time-dependent plastic effects to be diminished. The varied holding times in function C were used to investigate the effect of holding time.

Because of the heterogeneous properties of bone, its elastic properties were expected to exhibit differences for different microstructural components. Therefore, to minimize the effect of indent site, all the indents were made in osteonal lamellae. Even within a single osteon, a decline has been observed in both elastic modulus and hardness from the center of the osteon outward in mature secondary osteons.²⁰ Taking this into account, we chose locations having roughly equal radial distances to Haversian canals within the osteon

for each load function. Four indents were made in a 2×2 grid pattern $15 \mu\text{m}$ apart for each indentation rate or holding time. The indent depths of about 600 nm were produced with a peak load of 6 mN . The length of a side of an indent was approximately 7 times its depth, which was $4 \mu\text{m}$. Figure 2 shows an optical micrograph of the indents from load function A. Seven different indentation rates were used for functions A and B and eight different holding periods for function C, giving a total of 28 indents for functions A and B and a total of 32 indents for function C. Therefore, a total of 88 indents were made in this study.

In an indentation test, the deformed volume of material under the indenter is continually expanding to encompass previously undeformed material, which acts like an expanding elastic-plastic boundary. Because the radius of the elastic-plastic boundary often is related to the radius of the indentation, the instantaneous change in contact area divided by the instantaneous contact area (A'/A) is the most appropriate definition for the indentation strain rate, because it is a direct measure of the progression of the elastic-plastic boundary into the material.¹¹ For a geometrically similar indenter, such as the Berkovich indenter, the instantaneous displacement rate of the indenter divided by the instantaneous displacement (h'/h) is simply related to A'/A . The indentation strain rate is typically defined as h'/h . To obtain the indentation strain rate, the data of displacement and corresponding time were extracted from each indent and then curve fitted to the displacement-time function at the unloading portion. At the respective time point, the strain rate was calculated by taking the derivative of the function and dividing the derivative by the displacement at that point in time. Thus, each indentation strain rate was

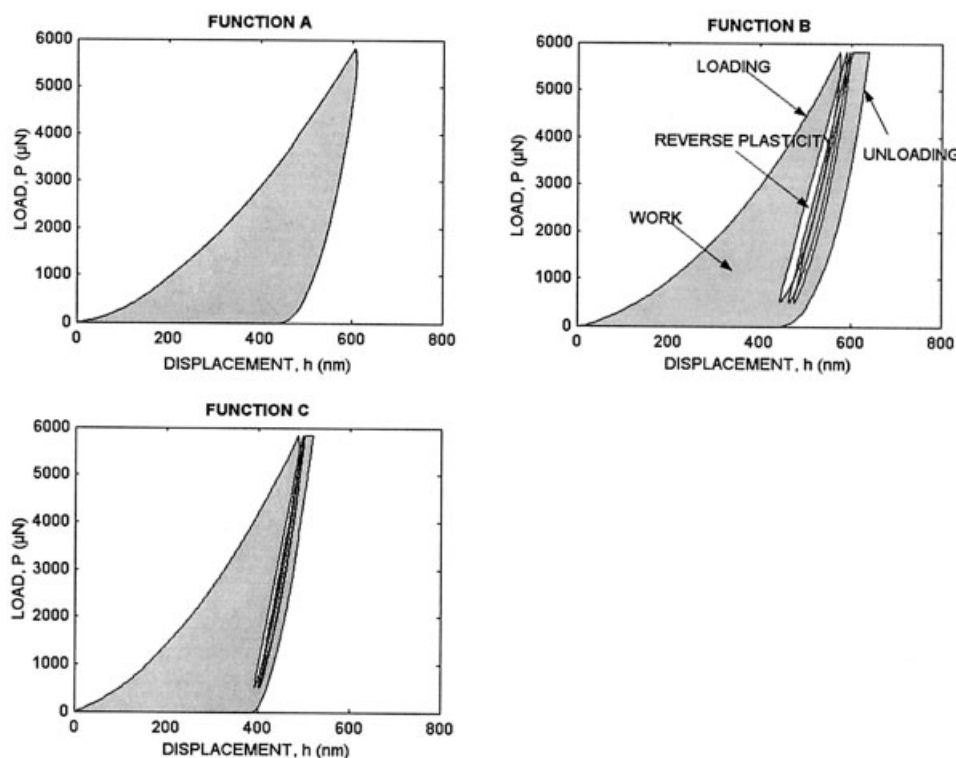


Figure 3. The load-displacement curves obtained from load functions A, B, and C.

TABLE I
The Elastic Modulus, Strain Rate, and Work Results
From Load Function A Regarding Different Indentation
Rates^a

Indentation Rate, $\mu\text{N/s}$	Elastic Modulus (GPa)	Strain Rate (μs^{-1})	Work ($\mu\text{N}\cdot\mu\text{m}$)
10	18.60 (0.92)	330 (90)	824.33 (69.30)
30	25.78 (1.90)	460 (50)	978.30 (54.96)
50	24.66 (0.41)	710 (100)	1069.35 (68.12)
100	26.50 (0.98)	1270 (140)	1056.05 (32.30)
300	26.92 (2.24)	4310 (320)	1041.19 (41.63)
500	28.91 (1.51)	6440 (680)	978.32 (52.67)
1000	32.22 (1.51)	13,560 (2360)	923.77 (33.50)

^aValues in parentheses indicate standard deviation.

calculated at the same data point where the contact stiffness (S) was determined.

The load-displacement curves obtained from the three load functions are shown in Figure 3. Some terms used in this study are illustrated in the curve of function B. Bone exhibits distinct hysteresis loops under multiple loading-unloading cycles, as might be expected if there were an amount of reverse plasticity upon unloading. The looping degenerates with loading-unloading cycling and is indistinguishable after three cycles. The displacement just before final unloading is due to creep and time-dependent plasticity. As shown in Figure 3, the shaded area between the first loading and the final unloading curves reflects the plastic deformation if the unloading data are assumed to be mostly elastic. This area is called "work" and is used to study the variations of plastic deformation with different load functions. The calculations of strain rate and work are all conducted with a program coded in Matlab 6.0 (MathWorks Inc., Natick, MA). To compare the work values for different indentation rates and holding periods, one-way analysis of variance (ANOVA) tests were performed, with $p < 0.05$ for significance. The Scheffé test (significance level of 5%) was used to determine whether specific pair-wise comparisons were significantly different. All statistical analyses were done with StatView 5.0.1 (SAS Institute Inc., Cary, NC).

RESULTS

Table I shows the results from load function A. As shown in this table, elastic modulus increased with increased indentation rates, which indicates that the measurement of elastic modulus using load function A is affected by viscoelasticity. With power regression, the elastic modulus and indentation strain rate were found to have the relationship:

$$E = 48.93(\dot{\epsilon})^{0.1002} \text{ with } R^2 = 0.70$$

where E is the elastic modulus and $\dot{\epsilon}$ is the indentation strain rate. The results of ANOVA test for works showed a significant difference among the different indentation strain rates for load function A ($p < 0.0001$).

TABLE II
The Elastic Modulus, Strain Rate, and Work Results
From Load Function B Regarding Different Indentation
Rates^a

Indentation rate, $\mu\text{N/s}$	Elastic Modulus (GPa)	Strain Rate (μs^{-1})	Work ($\mu\text{N}\cdot\mu\text{m}$)
10	22.69 (1.84)	305 (146)	1332.26 (234.24)
30	25.69 (1.12)	757 (74)	1198.27 (87.88)
50	26.10 (0.91)	1300 (142)	1147.51 (97.68)
100	26.34 (0.85)	2431 (125)	1292.65 (50.66)
300	27.91 (0.87)	7745 (265)	1381.79 (66.52)
500	29.30 (2.27)	12,463 (345)	1246.39 (74.15)
1000	30.38 (2.56)	25,151 (1094)	1250.01 (149.15)

^aValues in Parentheses indicate standard deviation.

Table II shows the results from load function B. The power regression indicated that the elastic modulus and strain rate have the relationship:

$$E = 37.74(\dot{\epsilon})^{0.0585} \text{ with } R^2 = 0.94$$

There was no significant difference among the different indentation strain rates for works in function B ($p = 0.24$).

Table III lists the results from load function C. The results of the ANOVA test revealed significant differences among the different holding times for works in load function C ($p < 0.01$). The Scheffé test indicated that the work from the 10-s holding period was significantly different from all of the other holding times, but all of the other holding times were not significantly different ($p = 0.27$). However, the differences among the elastic moduli at all holding times were not statistically significant ($p = 0.34$).

DISCUSSION

The indentation moduli of human cortical bone have been found to vary with different indentation rates, multiple loading-unloading cycles, and holding

TABLE III
The Elastic Modulus and Work Results From Load
Function C (Indentation Rate = 300 $\mu\text{N/s}$ and Peak
Load = 6000 μN) Regarding Various Holding Times at
Maximum Load^a

Holding Time's	Elastic Modulus (GPa)	Work ($\mu\text{N}\cdot\mu\text{m}$)
10	23.38 (1.27)	980.49 (94.60)
30	25.31 (3.12)	1148.85 (77.55)
50	26.76 (2.62)	1099.83 (36.39)
100	25.58 (0.33)	1152.16 (32.84)
180	24.85 (1.78)	1159.36 (21.69)
300	26.36 (0.71)	1142.74 (15.67)
500	25.76 (0.62)	1110.79 (36.11)
1000	26.57 (2.06)	1150.46 (40.87)

^aValues in Parentheses indicate standard deviation.

times at maximal load, which indicates that the viscoelasticity of cortical bone could be detected by nanoindentation techniques. Time-dependent mechanical properties can be measured by two techniques: 1. quasistatic techniques, in which the material response to different strain rates is measured or the strain rate is held constant while the material response is investigated; and 2. frequency-specific dynamic techniques, in which the load is varied at a single frequency and the response of the material is measured. In our study, quasistatic techniques were used to investigate the viscoelastic measurements and the effects of plasticity. In fact, the Oliver-Pharr method⁸ is based on the fully elastic recovery assumption. Multiple loading-unloading cycles and holding periods at maximal load frequently are used to minimize the contribution of plasticity to the unloading data.

During a nanoindentation test, bone materials usually exhibit a different manner from conventional mechanical testing in terms of plasticity. Bone materials express an obvious elastic portion at the beginning of conventional tests, such as tension and compression tests. The elastic properties of bone are usually investigated by analyzing the initial elastic deformation for conventional measurements. However, bone materials respond in an elastic-plastic manner in nanoindentation tests and plastic flow is usually described in terms of the elastic constraint offered by the surrounding material. The loading part of the indentation cycle consists of an initial elastic contact, followed by plastic flow, or yield within the specimen at higher loads. It was difficult to see an initial elastic contact portion with a Berkeovich indenter in bone materials because of the severe stress concentration that occurred (Fig. 3). Upon unloading, if yield has occurred, the load-displacement data follow a different path until load is completely removed and a residual impression is left in the specimen surface. During a plastic indentation, the bone material beneath the indenter experiences permanent compression in the direction perpendicular to the surface and radial expansion parallel to the surface. During the recovery, the stress normal to the surface is relieved, but the permanent radial expansion of the plastically deformed material induces a radial compressive stress exerted by the surrounding elastic material. In some cases, such as a spherical indenter on the high-modulus materials, it is possible to calculate the elastic modulus from not only the unloading curve, but also the loading portion of the curve because the initial loading portion of the indentation shows elastic.²¹ However, this is not the case in bone materials.

In conventional tests, Carter and Hayes⁶ found that elastic modulus was approximately proportional to strain rate raised to the 0.06 power. These relationships were suggested to be true for all bones in the

skeleton; however, our results from load function A do not support this hypothesis.

Many investigators have used conventional testing methods to evaluate viscoelastic properties in different types of bone.^{4,6,22} Most of these studies used the Ramberg-Osgood equation:

$$\epsilon = \frac{1}{c} T(\dot{\epsilon})^{-d} + a(T^n)(\dot{\epsilon})^{-b} \quad (3)$$

In this equation, ϵ is strain, $\dot{\epsilon}$ is strain rate, T is stress, and c , a , n , d and b are constants. The second term in this equation describes the plastic portion of a stress-strain curve, which is negligible for physiological levels of stresses. Thus, for the stresses and strains to which bone is normally exposed, the elastic modulus can be given as:

$$E = \frac{T}{\epsilon} = c(\dot{\epsilon})^d \quad (4)$$

However, because the load environment in nanoindentation testing is different from the physiological level, the plasticity effect cannot be ignored. As indicated in Table I, the work values, which reflect the plastic deformation during the indentation process, are significantly different among the different loading rates, suggesting that plasticity variations are due to changes in indentation rate and are time dependent. It was also observed that the work value increased with increased indentation rate until 50 $\mu\text{N/s}$ and then kept decreasing. In load function A, the tests with lower indentation rates lasted longer than the tests with higher indentation rates. Therefore, materials have more time to respond and exhibit more time-dependent plasticity, which is reflected by an increased work value. Meanwhile, when material has enough time to respond, there are also some occurrences of reverse plasticity, in which the total plasticity and the work value are reduced. The present study suggests that the up and down pattern seen in the work value results from the combined effects of time-dependent and reversed plasticity. Thus, plastic effects obviously exist in the unloading curve. Because of the fully elastic recovery assumption in the Oliver-Pharr method, the elastic modulus derived from load function A might not be reliable.

To minimize the contribution of plasticity in the unloading curve, load function B was used. Turnbull and White¹⁰ suggested that time-dependent plastic effects contributing to the unloading portion could result in an unsatisfactory analysis and that these effects could be eliminated with a sufficiently long holding time at maximal load. However, Lucas and Oliver¹¹ showed that hardness values were strongly affected by the holding time. In general, hardness measurements are done with short holding times to minimize creep effects. The assumption of constant

thermal drift becomes questionable when long holding times are used, so multiple loading–unloading cycles were used to reduce the creep effect and diminish the time-dependent plasticity. In the results from load function B, after multiple loading–unloading cycles and a 180-s holding period, the differences among the works for all indentation rates were not statistically significant, indicating that the plasticity variations caused by varying indentation rates were mostly diminished by the multiple loading–unloading cycles and holding time. The unloading curves are mostly composed of the elastic portion. Interestingly, the relationship between elastic modulus and indentation strain rate was found to be 0.059, which is quite similar to conventional test results.⁶ In previous studies of human bone,^{4,6,22,23} factor “*d*” in Equation 4 was found to range from 0.057 to 0.061. The result of 0.059 is well within this range. The constant “*c*” in Equation 4 is in the range of 15.2 to 24.5. The result from function B is 37.7. This discrepancy is attributed to the fact that the strain rate as determined by conventional tests may be proportional to the indentation strain rate.¹²

Whereas the holding period can minimize the plastic contribution to unloading data, hardness values are modulated by the creep effect. Therefore, it was necessary to find a compromise in selecting an appropriate value for the holding time. Load function C was designed for this purpose. Multiple loading–unloading cycles can reduce the effect of plasticity without producing much creep problem. Thus, in function C, the holding time was varied after three loading–unloading cycles to reduce the time-dependent plastic effect. There was no difference in the work for the various holding periods, except the 10-s holding period. Although the 10-s holding time was not sufficient to diminish the time-dependent plastic effect in this study, a holding period of 30 s is long enough to obtain most elastic unloading data. However, differences among the elastic moduli at all holding times were not statistically significant. Because all indents conducted in this load function had the same loading rate, it was unexpected that the elastic modulus obtained from the 10-s holding period was not different from the others. This may be attributed to local variations within osteonal lamella.

Although nanoindentation has been used to investigate the microstructural properties of bone material, the effects of viscoelastic and time-dependent plastic properties on nanoindentation measurements have not been defined. Quasi-static nanoindentation analysis is based on an assumption of fully elastic recovery without consideration of viscoelasticity and time-dependent plasticity. Therefore, load-time functions should be designed carefully when nanoindentation testing is applied to bone material. From the experiments with designed load-time functions, a power relationship was found between the elastic modulus

and indentation strain rate. When the contribution of plasticity to unloading data is taken into account, this power relationship is surprisingly similar to previous results obtained from conventional testing methods.

Human cortical bone has a very complicated structure and its mechanical properties are dependent on many factors. Different microstructures, anatomy locations, diseases, gender, and age have been suggested to affect mechanical measurements of human cortical bone. How these factors influence the viscoelasticity of cortical bone has not been explored systematically. In our study, we investigated the viscoelasticity of only osteonal lamellae, but the results indicate that carefully designed nanoindentation studies can measure the viscoelastic properties of bone. In daily activities, human cortical bone undergoes dynamic loading and strain-rate changes. Strain-rate variations often are considered to be a signal that triggers many biological activities of bone remodeling.²⁴ Some defects of human cortical bone result from repetitive dynamic loading and are initialized at the microstructural level. Therefore, a better understanding of the viscoelastic properties of bone microstructure is important in understanding many clinical and research problems.

REFERENCES

1. Rho JY, Spearing-Kuhn L, Zioupos P. Mechanical properties and the hierarchical structure of bone. *Med Eng Phys* 1998;20: 92–102.
2. Weiner S, Wagner HD. The material bone: structure-mechanical function relations. *Annu Rev Mater Sci* 1998;28:271–298.
3. Sasaki N, Yoshikawa M. Stress relaxation in native and EDTA-treated bone as a function of mineral content. *J Biomech* 1993; 26:77–83.
4. McElhaney JH. Dynamic response of bone and muscle tissue. *J Appl Physiol* 1966;21:1231–1236.
5. Carter DR, Hayes WC. Bone compressive strength: the influence of density and strain rate. *Science* 1976;194:1174–1176.
6. Carter DR, Hayes WC. The compressive behavior of bone as a two-phase porous structure. *J Bone Joint Surg Am* 1977;59:954–962.
7. Rho JY, Pharr GM. Effects of drying on the mechanical properties of bovine femur measured by nanoindentation. *J Mater Sci Mater Med* 1999;10:1–4.
8. Oliver WC, Pharr GM. An improved technique for determining hardness and elastic modulus using load and displacement sensing indentation experiments. *J Mater Res* 1992;7:1564–1583.
9. Flores A, Calleja FJB. Mechanical properties of poly(ethylene terephthalate) at the near surface from depth-sensing experiments. *Philos Mag A* 1998;78:1283–1297.
10. Turnbull A, White D. Nanoindentation and microindentation of weathered UPVC. *J Mater Sci* 1996;31:4189–4198.
11. Lucas BN, Oliver WC. Indentation power-law creep of high-purity indium. *Metal Mater Trans A* 1999;30A:601–610.
12. Pollock HM, Maugis D, Barquins M. Characterization of sub-micrometer surface layers by indentation. In: Blau PJ, Lawn BR, editors. *Microindentation techniques in materials science and engineering*, ASTM STP 889. Philadelphia: ASTM; 1986. p 47–71.

13. Hengsberger S, Kulik A, Zysset P. Nanoindentation discriminates the elastic properties of individual human bone lamellae under dry and physiological conditions. *Bone* 2002;30:178–184.
14. Rho JY, Tsui TY, Pharr GM. Elastic properties of human cortical and trabecular lamellar bone measured by nanoindentation. *Biomaterials* 1997;18:1325–1330.
15. Rho JY, Roy ME, Tsui TY, Pharr GM. Elastic properties of microstructural components of human bone tissue as measured by nanoindentation. *J Biomed Mater Res* 1999;45:48–54.
16. Zysset PK, Guo XE, Hoffer CE, Moore KE, Goldstein SA. Elastic modulus and hardness of cortical and trabecular bone lamellae measured by nanoindentation in the human femur. *J Biomech* 1999;32:1005–1012.
17. Hoffer CE, Moore KE, Kozloff K, Zysset PK, Brown MB, Goldstein SA. Heterogeneity of bone lamellar-level elastic moduli. *Bone* 2000;28:603–609.
18. Zysset PK, Guo XE, Hoffer CE, Moore KE, Goldstein SA. Mechanical properties of human trabecular bone lamellae quantified by nanoindentation. *Technol health Care* 1998;6(5–6):429–432.
19. Fondrk M, Bahniuk E, Davy DT, Michaels C. Some viscoplastic characteristics of bovine and human cortical bone. *J Biomech* 1988;21:623–630.
20. Rho JY, Zioupos P, Currey JD, Pharr GM. Variations in the individual thick lamellar properties within osteons by nanoindentation. *Bone* 1999;25:295–300.
21. Kramer D, Huang H, Kriese M, Robach J, Nelson J, Wright A, Bahr D, Gerlicher WW. Yield strength predictions from the plastic zone around nanocontacts. *Acta Mater* 1999;47:333–343.
22. Hight TK, Brandeau JF. Mathematical modeling of the stress strain-strain rate behavior of bone using the Ramberg-Osgood equation. *J Biomech* 1983;16:445–450.
23. Wood JL. Dynamic response of human cranial bone. *J Biomech* 1971;4:1–12.
24. Roesler H. Some historical remarks on the theory of cancellous bone structure (Wolff's law). In: Cowin SC, editor. *Mechanical properties of bone*. New York: American Society of Mechanical Engineers; 1981. p 27–42.